Two Schiff-base complexes of copper and zirconium oxide supported on mesoporous MCM-41 as an organic–inorganic hybrid catalysts in the chemo and homoselective oxidation of sulfides and synthesis of tetrazoles

Mohsen Nikoorazm[1] [iD] · **Ziba Rezaei**[1] · **Bahman Tahmasbi**[1]

Abstract

A simple and efficient procedure was reported for the synthesis of tetrazole derivatives, the chemo and homoselective oxidation of sulfides to sulfoxides in the presence of two Schiff-base complexes of zirconium oxide and copper anchored on MCM-41 as mesoporous and organometallic catalysts under green conditions. All the products were obtained in excellent yields with high TOF values indicating the high activity of the synthesized catalysts. These catalysts were characterized by XRD, TGA, SEM, EDS, FT-IR, TEM, WDX, BET and AAS techniques and can be recycled for several times without significant loss in catalytic activity. The recovered catalysts were characterized by SEM, FT-IR and AAS analysis which shown an excellent agreement with fresh catalysts.

Keywords Mesoporous MCM-41 · Schiff-base · Tetrazoles · Chemoselective oxidation · Homoselective oxidation

1 Introduction

Catalytic processes play an important role in the chemical and pharmaceutical industries [1–10]. The recoverability and recyclability of the catalysts are great factors in catalytic science [11–15]. Homogeneous catalysts have several limitations such as purification of the final products, recovering and reusing of the catalyst [16]. These limitations can be overcome by heterogenization of homogeneous catalysts using immobilization of homogeneous catalysts on various solid materials [17–19]. In order to combine the advantages of both homogeneous (high selectivity and activity) and heterogeneous (stability and reusability) catalysts, nanomaterials such as carbon nanotubes [23], polymers [24], ionic liquids [25, 26], iron oxide [27], graphene oxide [28, 29], silica materials [30], boehmite nanoparticles [31, 32] and

✉ Mohsen Nikoorazm
   e_nikoorazm@yahoo.com

1   Department of Chemistry, Faculty of Science, Ilam
   University, P.O. Box 69315516, Ilam, Iran

etc. have been widely used as the great and useful supports for the immobilization of homogeneous catalysts [20–22]. Among the various nanomaterials, the preparation of nanostructured porous silicate such as MCM-41 has been greatly explored as support catalysts. MCM-41 have recently been used in various fields, such as extraction [33], catalysis [34], drug delivery systems [35], energy [36] and adsorption [37]. Also, MCM-41 has been used in the recovering and recycling of expensive homogeneous catalysts [38]. MCM-41 has unique properties such as homogeneous hexagonal pore (with 1.5–10 nm of pore diameters), large specific surface area (> 1000 m^2/g), ease of functionalization, relatively hydrophobic nature, high thermal stability (900 °C) and simple preparation and separation [39, 40]. High specific pore volumes (up to 1.3 mL/g) of MCM-41 allow immobilization of the large molecules such as metallic complexes into channels [41]. Existence of many surface silanol groups and large surface area could be functionalized with different compounds such as metal complexes. Therefore, covalent anchoring of the supported catalysts onto MCM-41 combined with high thermal stability of MCM-41 which allows organic reactions to proceed in high temperatures [42–46]. To extend the application of active heterogeneous catalysts, we would like to report synthesis and characterization of

Scheme 1 Synthesis of Schiff-base compound (SB-APT) as ligand
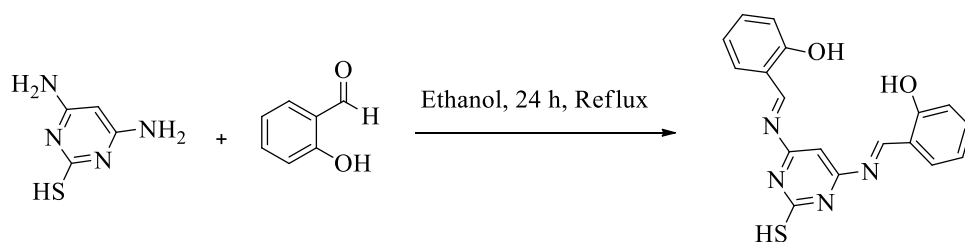
Schiff-base complexes of zirconium oxide and copper catalysts on MCM-41 as efficient and recyclable catalyst for the synthesis of tetrazoles and the chemo and homoselective oxidation of sulfides to sulfoxides.

2 Experimental

2.1 Preparation of catalyst

Initially, Schiff-base compound (SB-APT) has been synthesized by stirring of 4,6-diaminopyrimidine-2-thiol (1 mmol) and salicylaldehyde (2 mmol) in ethanol for 24 h under reflux conditions; Scheme 1. This ligand has been characterized by ^{1}H NMR and FT-IR technique as: ^{1}H NMR (250 MHz, DMSO): $\delta_H = 10.97$ (s, 2H), 6.57 (br, 9 H), 5.01 (br, 2H), 2.48 (s, 1H) ppm.

IR (KBr) cm^{-1}: 3436, 3392, 3253, 3061, 2921, 2856, 2717, 1645, 1627, 1564, 1424, 1313, 1251, 1198, 1018, 971, 942, 862, 785, 638, 552, 513, 459.

The modified MCM-41 by CPTMS (Cl@MCM-41) was prepared according to the reported procedure [47]. Then, Cl@MCM-41 (1 g) was dispersed in 25 mL toluene, and then SB-APT (3 mmol) was added to the reaction mixture and stirred for 72 h at 100 °C. Then, the resulting powder (SB-APT@MCM-41) was filtered, washed with ethanol and dried at 50 °C. Finally, SB-APT@MCM-41 (1 g) was dispersed in 25 mL ethanol, and then ZrOCl$_2$·8H$_2$O (3 mmol) or Cu(NO$_3$)$_2$·9H$_2$O (3 mmol) were added to the reaction mixture and was stirred magnetically for 20 h under reflux conditions. The obtained catalysts (Cu-SB-APT@MCM-41) or (ZrO-SB-APT@MCM-41) were filtered and washed with ethanol and water.

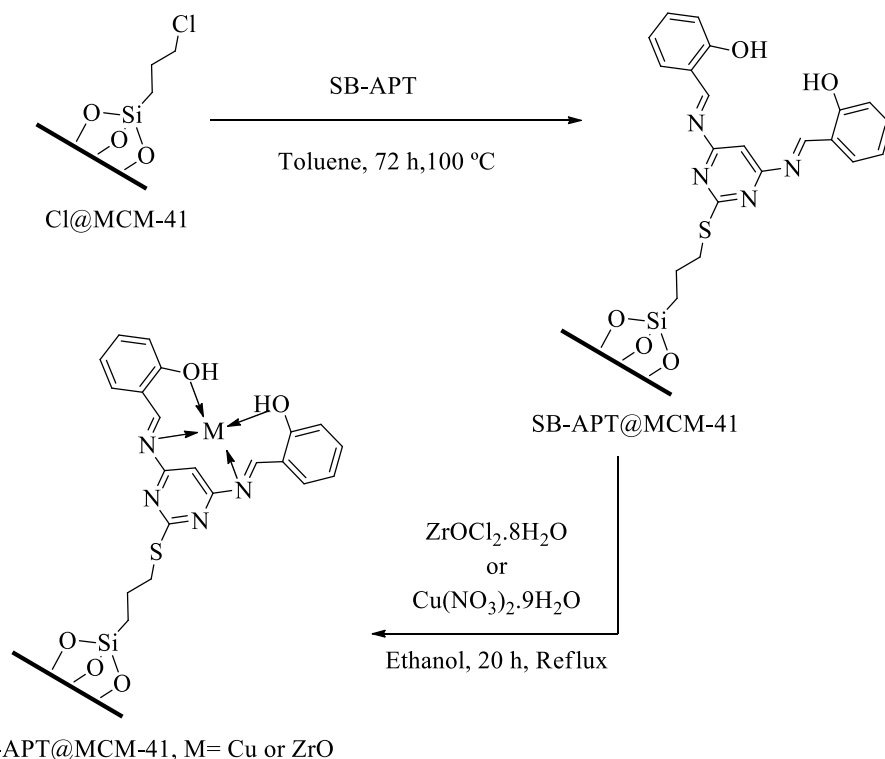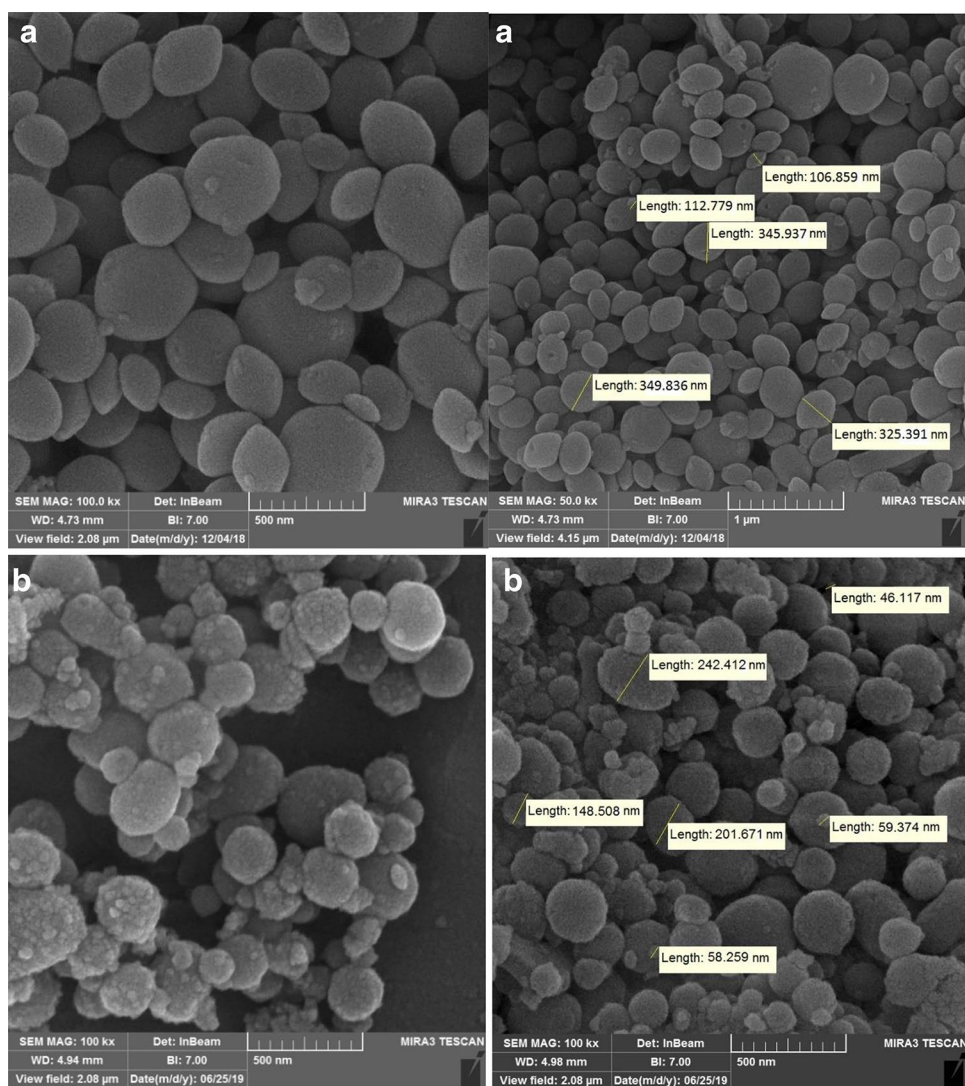**Scheme 2** Preparation of Cu-SB-APT@MCM-41 and ZrO-SB-APT@MCM-41

M-SB-APT@MCM-41, M= Cu or ZrO

Fig. 1 SEM images of Cu-SB-APT@MCM-41 (**a**) and ZrO-SB-APT@MCM-41 (**b**)

2.2 General procedure for the synthesis of 5-substituted 1H-tetrazoles

A mixture of NaN$_3$ (1.5 mmol) and benzonitrile derivative (1 mmol) in the presence of Cu-SB-APT@MCM-41 (0.025 g) or ZrO-SB-APT@MCM-41 (0.030 g), were stirred at 120 °C in poly ethylene glycol (PEG-400) as solvent. After completion of the reaction (indicated by TLC), the catalyst was isolated by simple filtration and the products were extracted by aqueous solution of HCl (4 N) and ethyl acetate. The organic solvent was dried over anhydrous sodium sulfate and concentrated to give the crude solid product.

2.3 General procedure for the oxidation of sulfides to sulfoxides

Sulfide derivatives (1 mmol) and 0.5 mL of H$_2$O$_2$ (33%) were added to 0.0025 g of Cu-SB-APT@MCM-41 in ethyl acetate or 0.02 g of ZrO-SB-APT@MCM-41 under solvent-free conditions and the mixture was stirred at room temperature. The progress of the reaction was monitored by TLC. After completion of the reaction, the catalyst was separated by simple filtration and the products were extracted with water and ethyl acetate. The organic layer was dried over
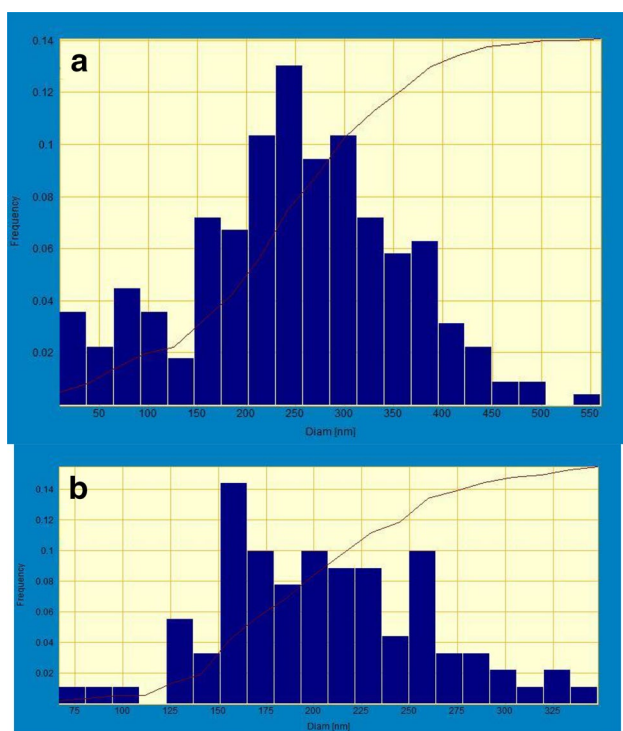
Fig. 2 Particle size distribution histogram of Cu-SB-APT@MCM-41 (**a**) and ZrO-SB-APT@MCM-41 (**b**)

anhydrous Na_2SO_4 and then was evaporated to obtain the pure products.

2.4 Selected spectral data

1-(4-(1H-tetrazol-5-yl)phenyl)ethanone: ^{1}H NMR (250 MHz, $CDCl_3$): δ_H = 8.25–8.13 (d, J = 30 Hz, 2 H), 7.71–7.53 (d, J = 45 Hz, 2 H), 2.68 (s, 3H) ppm; IR (KBr) cm^{-1}: 3071, 3009, 2921, 2854, 1684, 1568, 1532, 1402, 1357, 1265, 1158, 1082, 1055, 1018, 992, 962, 873, 751, 726, 700, 616, 591, 562, 560, 420.

(sulfinylbis(methylene))dibenzene: ^{1}H NMR (400 MHz, DMSO): δ_H = 7.36–7.31 (m, 10 H), 4.19–4.14 (d, J = 12 Hz, 2 H), 3.89–3.85 (d, J = 12 Hz, 2 H) ppm; IR (KBr) cm^{-1}: 2925, 2854, 1737, 1637, 1620, 1491, 1454, 1411, 1384, 1281, 1132, 1073, 1031, 918, 887, 615, 589, 498, 472.

(benzylsulfinyl)benzene: ^{1}H NMR (400 MHz, DMSO): δ_H = 7.52–7.46 (m, 5 H), 7.28–7.20 (m, 3 H), 7.07–7.03 (m, 2 H), 4.26–4.21 (d, J = 12 Hz, 1 H), 4.07–4.02 (d, J = 12 Hz, 1 H) ppm; IR (KBr) cm^{-1}: 2958, 2854, 1737, 1634, 1582, 1491, 1448, 1413, 1282, 1124, 1071, 1036, 996, 914, 890, 767, 692, 616, 545, 494, 477.
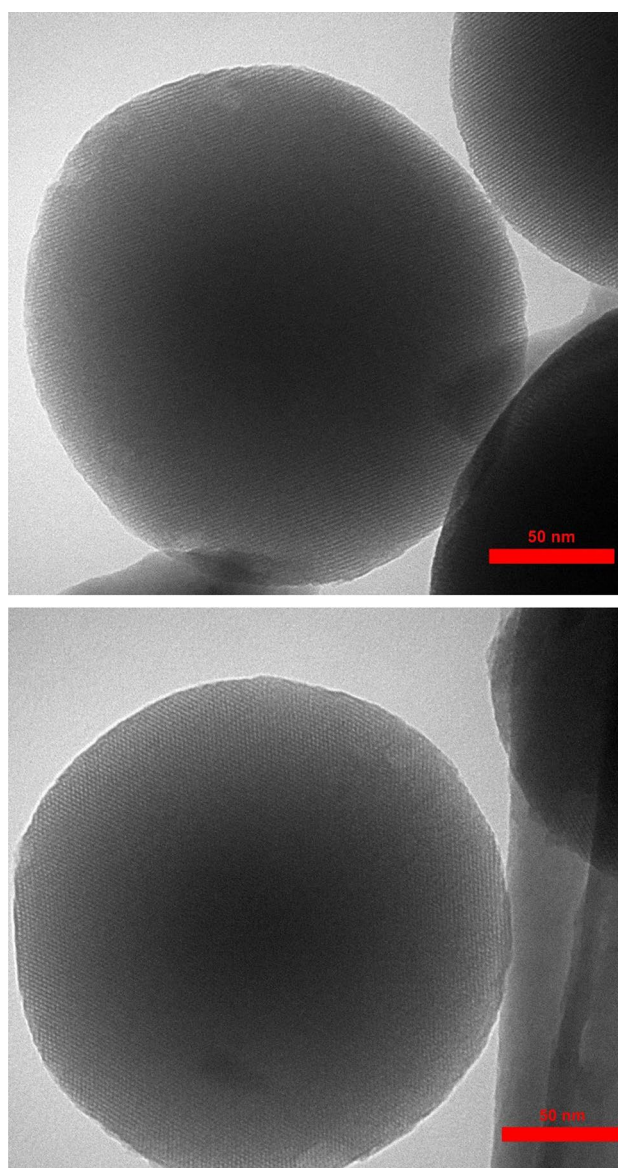

Fig. 3 TEM images of Cu-SB-APT@MCM-41

3 Results and discussion

3.1 Catalyst preparation and identification

In this work, two Schiff-base complexes of copper and zirconium on mesoporous MCM-41 and their application as a reusable catalyst for organic reactions were reported. For preparation of these catalysts, the modified MCM-41 nanoparticles with 3-choloropropyltriethoxysilane (CPTES) has been synthesized according to the reported procedure [47].

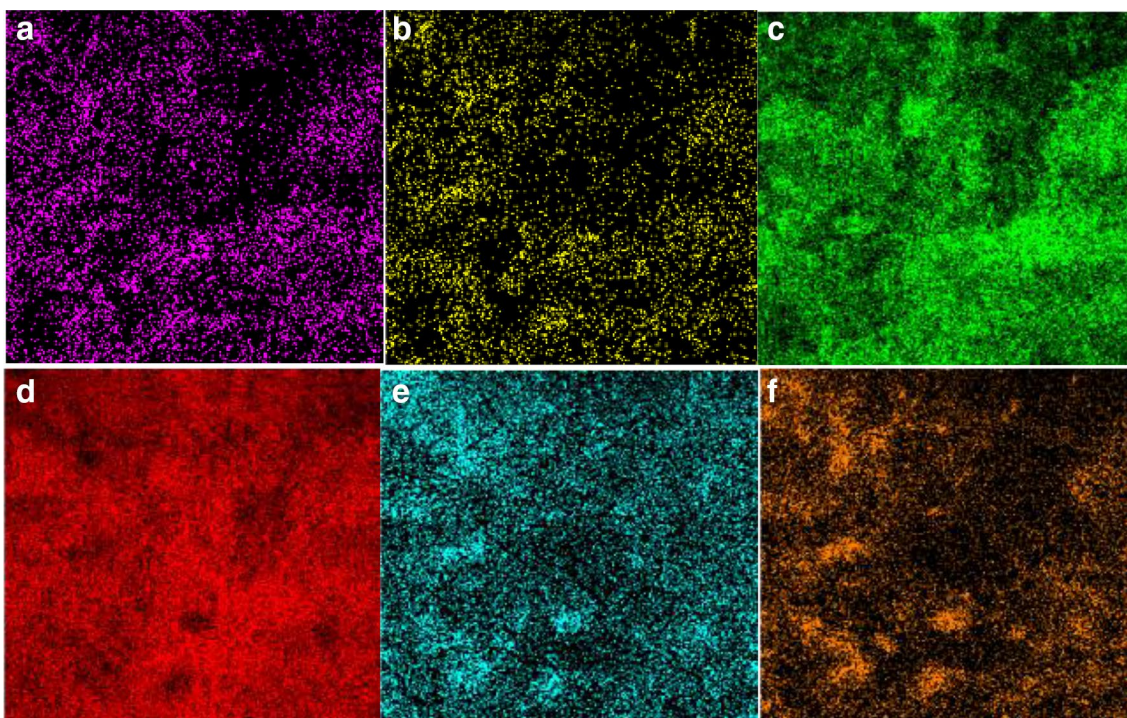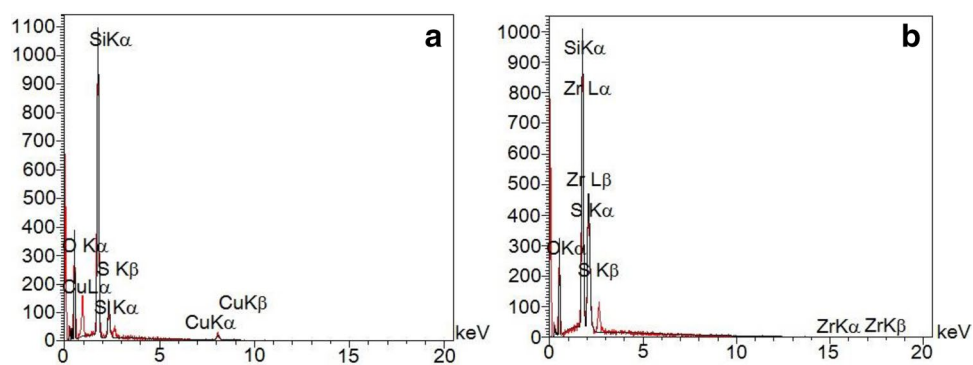**Fig. 4** EDS diagrams of Cu-SB-APT@MCM-41 (**a**) and ZrO-SB-APT@MCM-41 (**b**) (Color figure online)

Fig. 5 Elemental mapping of (**a**) carbon, (**b**) nitrogen, (**c**) oxygen, (**d**) silica, (**e**) sulfur, and (**f**) copper for Cu-SB-APT@MCM-41

In order to immobilize the Schiff-base ligand on the surface of obtained nanoparticles, the terminal chorine groups were reacted with SB-APT. Finally, zirconium or copper ions were stabilized on SB-APT@MCM-41 (Scheme 2). These nanocatalysts were characterized by scanning electron microscopy (SEM), wavelength dispersive X-ray spectroscopy (WDX), energy-dispersive X-ray spectroscopy (EDS), transmission electron microscopy (TEM), Fourier transform infrared spectroscopy (FT-IR), N_2 adsorption–desorption isotherms, thermogravimetric analysis (TGA), X-ray diffraction (XRD), and atomic absorption spectroscopy (AAS) techniques.

3.2 Catalyst characterization

SEM technique was used to get information about the morphology and particles size of the catalysts. The SEM images of Cu-SB-APT@MCM-41 and ZrO-SB-APT@MCM-41 were shown in Fig. 1. The morphology of samples was
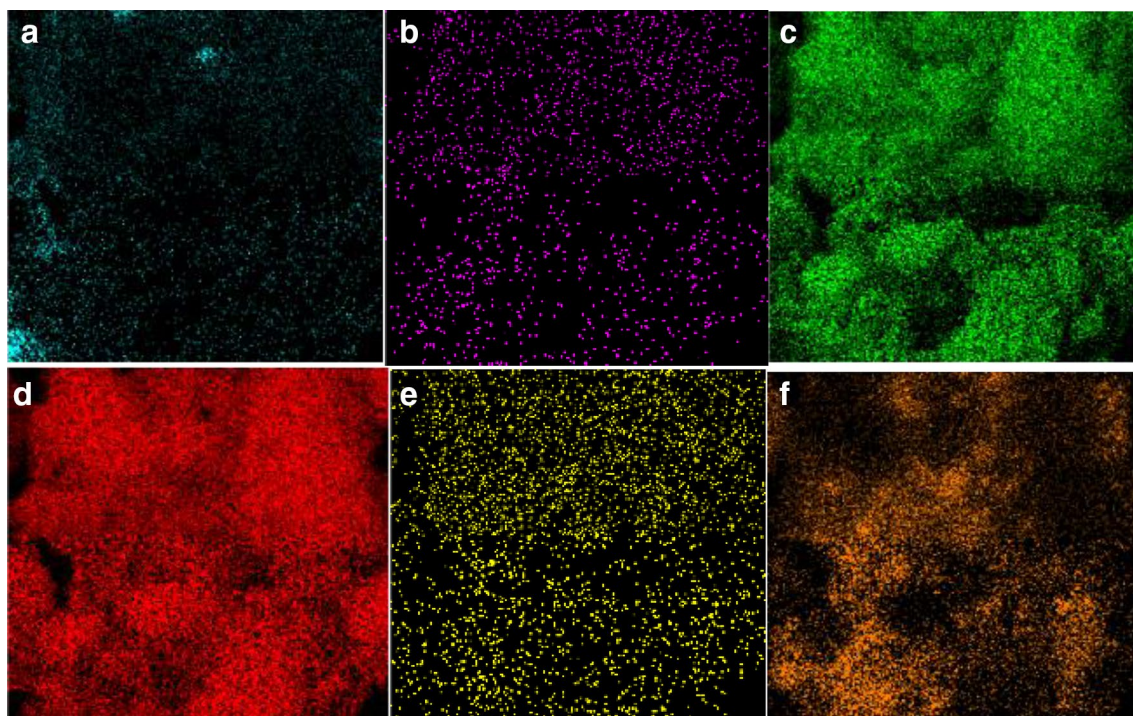
Fig. 6 Elemental mapping of (**a**) carbon, (**b**) nitrogen, (**c**) oxygen, (**d**) silica, and (**e**) sulfur, and (**f**) zirconium for ZrO-SB-APT@MCM-41
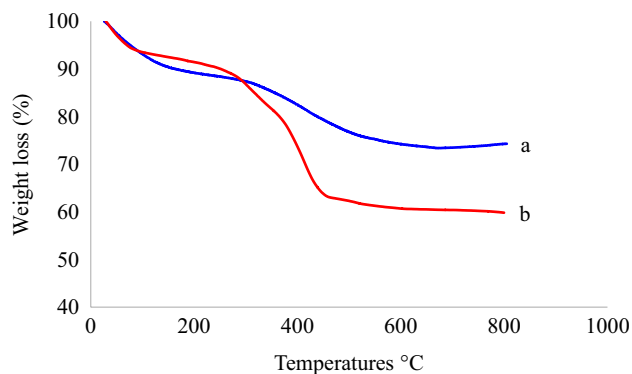

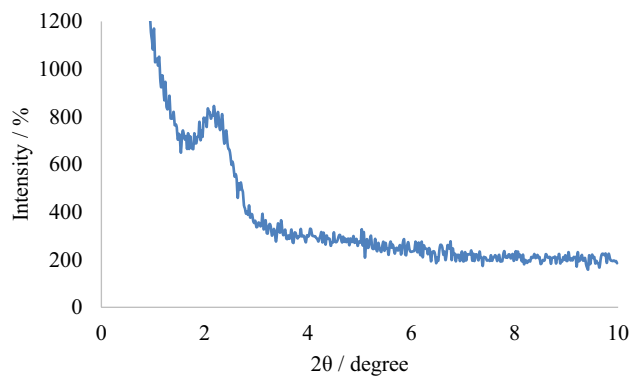**Fig. 7** TGA diagrams of ZrO-SB-APT@MCM-41 (a) and Cu-SB-APT@MCM-41 (b)

Fig. 8 The low XRD pattern of ZrO-SB-APT@MCM-41

found to be uniform spherical with a mean diameter less than 500 nm. To indicate the Particle size distribution of these catalysts, the histogram of particles size which have been obtained from SEM images are shown in Fig. 2.

Also, TEM images of Cu-SB-APT@MCM-41 is shown in Fig. 3. As it can be seen the morphology of particles

shown a good similarly to indicate particles in SEM images of this catalyst. Also, particles size of Cu-SB-APT@MCM-41 in TEM images are shown a good similarly to obtained its particle size form SEM images. More importantly, highly ordered long-range hexagonal arrangement of the
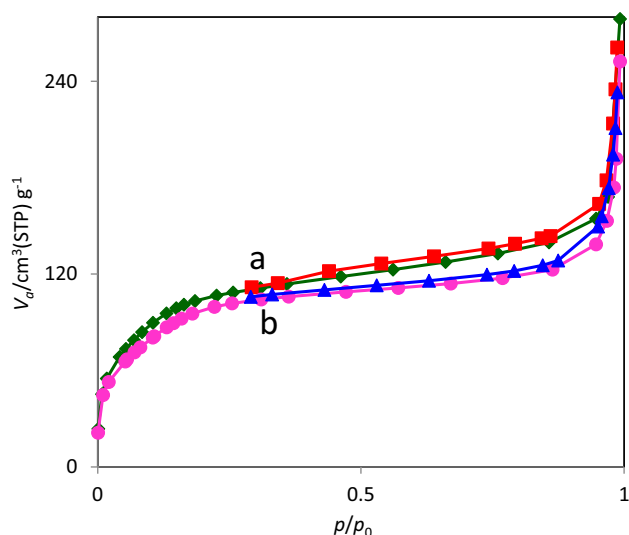
Fig. 9 N$_2$ adsorption–desorption isotherm of ZrO-SB-APT@MCM-41 (a) and Cu-SB-APT@MCM-41 (b)

mesoporous channels were clearly observed in TEM images of Cu-SB-APT@MCM-41.

The elements content of the catalysts were determined using EDS analysis. EDS diagrams of Cu-SB-APT@MCM-41 and ZrO-SB-APT@MCM-41 are shown in Fig. 4. As depicted, the EDS result of Cu-SB-APT@MCM-41 shows the presence of oxygen, silica, carbon, sulfur, nitrogen and copper species in the structure of this catalyst. Also, the EDS diagram of ZrO-SB-APT@MCM-41 indicates the presence of oxygen, silica, carbon, sulfur, nitrogen and as well as zirconium species. These results are shown a good agreement with the structure of catalysts that are shown in Scheme 1. The black and red lines in EDS diagrams are

correspond to the calibration curve and obtained results from the catalysts, respectively. As shown in Fig. 4, a good agreement was observed between the calibration curve and obtained results from the catalysts which were confirmed the high purity of described catalysts. The EDS results of Cu-SB-APT@MCM-41 and ZrO-SB-APT@MCM-41 were extended by WDX analysis which is shown in Figs. 5 and 6. As shown in Figs. 5 and 6, a homogeneous distribution of all elements contained in the structure of these catalysts was clearly observed.

Also, the exact amounts of copper (in Cu-SB-APT@MCM-41) or zirconium (in ZrO-SB-APT@MCM-41) were found to be 2.2×10^{-3} and 0.076×10^{-3} mol g^{-1}, respectively.

Figure 7 belongs to TGA curves of ZrO-SB-APT@MCM-41 and Cu-SB-APT@MCM-41. The small mass loss about 10% (for TGA curve of ZrO-SB-APT@MCM-41, Fig. 7a) and 9% (for TGA curve of Cu-SB-APT@MCM-41, Fig. 7b) at low temperatures (below 200 °C) is associated to the evaporation of adsorbed solvents [48, 49]. Also, the second mass loss in TGA diagrams of ZrO-SB-APT@MCM-41 (about 17 wt%) and Cu-SB-APT@MCM-41 (about 31 wt%) between 200 and 600 °C corresponded to the calcination of immobilized organic groups on MCM-41 nanoparticles [31]. The final mass loss above 600 °C, that is 1 wt% and 2 wt% loss for ZrO-SB-APT@MCM-41 and Cu-SB-APT@MCM-41 respectively is related to the condensation of the silanol groups of MCM-41 [16].

Given that the wide range of organic compounds are usually synthesized in high temperature, thermal stability of ZrO-SB-APT@MCM-41 and Cu-SB-APT@MCM-41 was also confirmed by TGA analysis. Based on TGA diagrams of these catalysts, no weight loss was observed up to 250 °C (except the removal of solvents). As shown in Fig. 7,

Table 1 Textural properties of MCM-41, ZrO-SB-APT@MCM-41 and Cu-SB-APT@MCM-41

Entry	Sample	S$_{BET}$ (m^2/g)	Pore diameter (nm)	Pore volume (cm^3 g^{-1})
1	MCM-41	1113.7 [50]	2.45 [34]	1.39 [50]
2	ZrO-SB-APT@MCM-41	112.1	1.22	0.30
3	Cu-SB-APT@MCM-41	113.9	1.29	0.27

Fig. 10 FT-IR spectra of MCM-41 (a), Cl@MCM-41 (b), SB-APT@MCM-41 (c), Cu-SB-APT@MCM-41 (d) and ZrO-SB-APT@MCM-41 (e)
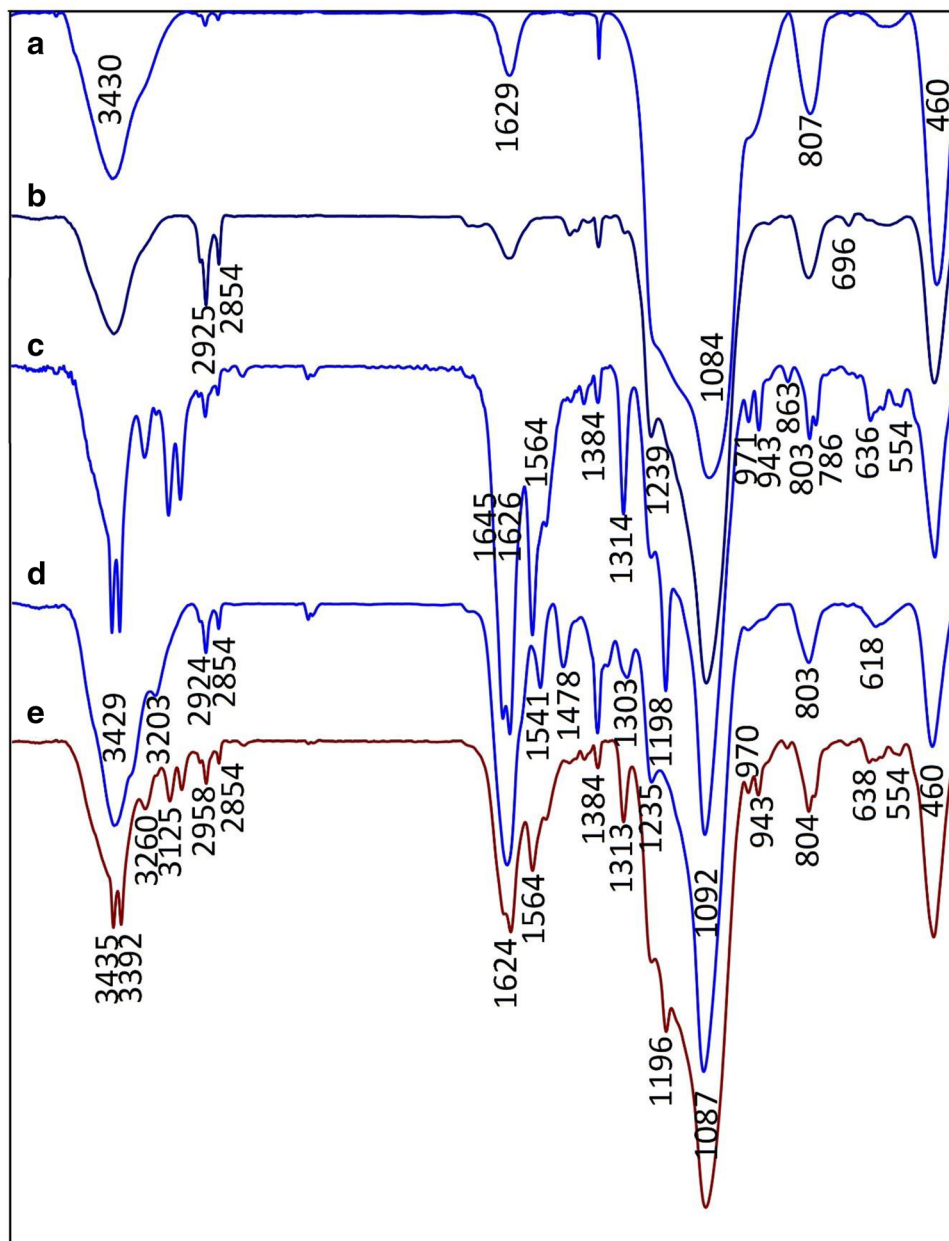
Scheme 3 Synthesis of 5-substituted 1H-tetrazoles in the presence of ZrO-SB-APT@MCM-41 or Cu-SB-APT@MCM-41
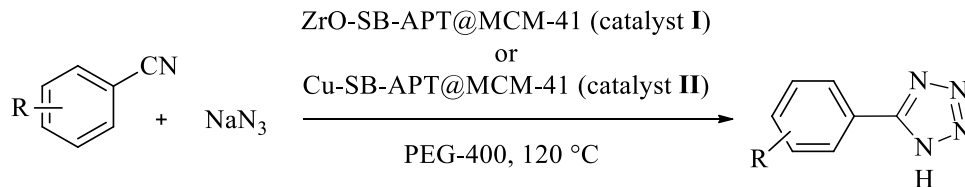
Table 2 Optimization reaction conditions for the synthesis of tetrazoles in the presence of ZrO-SB-APT@MCM-41 (catalyst I) or Cu-SB-APT@MCM-41 (catalyst II)

Entry	Catalyst	Amount of catalyst (mg)	Solvent	Temperature (°C)	Time (min)	Yield (%)[a]
1	–	–	PEG	120	240	–[b]
2	Catalyst **I**	20	PEG	120	215	58
3	Catalyst **I**	30	PEG	120	130	86
4	Catalyst **I**	40	PEG	120	60	92
5	Catalyst **I**	40	Toluene	120	?	?
6	Catalyst **I**	30	H_2O	100	240	51
7	Catalyst **I**	30	DMSO	120	180	80
8	Catalyst **I**	30	PEG	100	150	62
9	Catalyst **I**	30	PEG	80	210	49
10	Catalyst **II**	15	PEG	120	140	55
11	Catalyst **II**	20	PEG	120	115	64
12	Catalyst **II**	25	PEG	120	55	92
13	Catalyst **II**	25	H_2O	100	240	59
14	Catalyst **II**	25	DMSO	120	180	82
15	Catalyst **II**	25	Toluene	120	260	47
16	Catalyst **II**	25	Dioxane	120	215	53
17	Catalyst **II**	25	PEG	100	120	70
18	Catalyst **II**	25	PEG	80	210	50

[a]Isolated yield, [b]No reaction

ZrO-SB-APT@MCM-41 and Cu-SB-APT@MCM-41 are stable even to 250 °C.

The small- angle powder XRD pattern for ZrO-SB-APT@MCM-41 is shown in Fig. 8. The low angle XRD pattern of ZrO-SB-APT@MCM-41shows the peak at 2θ = 2.26° and also two weak peaks at 2θ = 4.08° and 5.14° which are related to 1 0 0, 1 1 0 and 2 0 0 diffraction plans, respectively. All the obtained results are in good agreement with standard XRD pattern of MCM-41 with the hexagonal unit cell of channels [38]. The decreasing intensity of the peaks at 2θ = 4.08° and 5.14° is due to immobilization of organic layers and zirconium complex in MCM-41 channels [16].

The N_2 adsorption–desorption isotherms of ZrO-SB-APT@MCM-41 and Cu-SB-APT@MCM-41 are shown in Fig. 9 which display typical type IV isotherms related to characteristic of mesoporous materials based on the IUPAC classification [47]. Also, textural properties of MCM-41, ZrO-SB-APT@MCM-41 and Cu-SB-APT@MCM-41 are summarized in Table 1 which is determined from N_2 adsorption–desorption analysis. As shown in Table 1, surface area, pore volumes and pore diameters of ZrO-SB-APT@MCM-41 are 112.1 m^2 g^{-1}, 0.30 cm^3 g^{-1} and 1.22 nm respectively. Also, surface area, pore volumes and pore diameters of Cu-SB-APT@MCM-41 are 113.9 m^2 g^{-1}, 0.27 cm^3 g^{-1} and 1.29 nm respectively. In comparison to the textural properties of MCM-41 (Table 1, entry 1), decreasing in surface area, pore volumes and pore diameters of

Ni- ZrO-SB-APT@MCM-41 and Cu-SB-APT@MCM-41 are due to the grafting of organic layers and metal complexes into channels of MCM-41 [16].

The FT-IR spectra of MCM-41, Cl@MCM-41, SB-APT@MCM-41, ZrO-SB-APT@MCM-41 and Cu-SB-APT@MCM-41 are outlined in Fig. 10. In FT-IR spectrum of mesoporous MCM-41, three peaks at 460, 807, and 1084 cm^{-1} corresponded to the Si–O–Si vibrations [16] indicated these bands are present in all the FT-IR spectra. Also, stretching vibrational modes at (2925 and 2854 cm^{-1}) and (696 cm^{-1}) in the FT-IR spectrum of Cl@MCM-41 is associated to the C–H and C–Cl bonds, confirmed modification of the MCM-41 by CPTMS [27] which are not indicate in FT-IR spectra of MCM-41. Several peaks at 1645, 1564, 1313, 1198, 971, 942, 862, 785, 638 and 552 cm^{-1} in FT-IR spectrum of SB-APT@MCM-41 confirmed that SB-APT was successful supported on MCM-41.

3.3 Catalytic activity

After synthesis and characterization of catalysts, our studies were directed towards the investigation of the catalytic activity of ZrO-SB-APT@MCM-41 and Cu-SB-APT@MCM-41 for chemical synthesis of the tetrazole derivatives (Scheme 3) and the chemo and homoselective oxidation of sulfides to sulfoxides (Scheme 3).

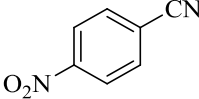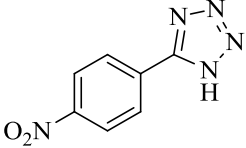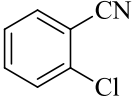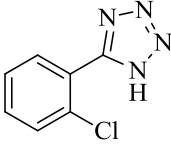**Table 3** Synthesis of tetrazoles in the presence of ZrO-SB-APT@MCM-41
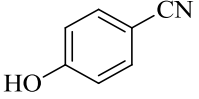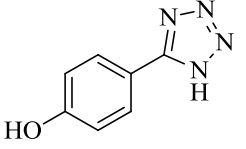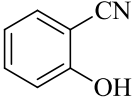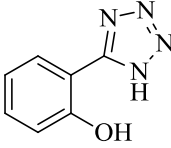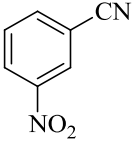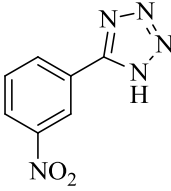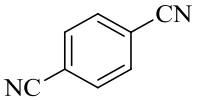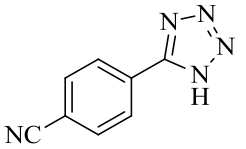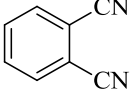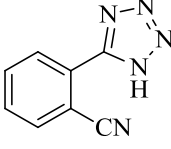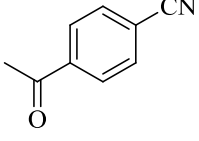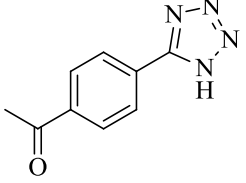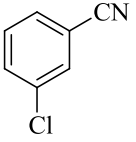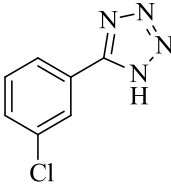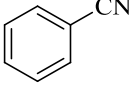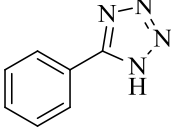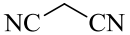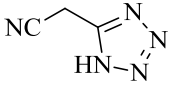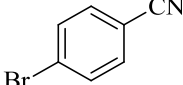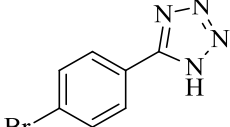
Entry	Nitrile	Product	Time (min)	TON	TOF (h^{-1})	Yield[a] (%)	Obtained Melting point (°C)	Reported Melting point (°C)
1			60	408.7	408.7	94	221–223	220–221 [47]
2			130	378.3	174.6	87	183–185	180–183 [31]
3			100	391.3	234.8	90	233–234	233–235 [31]
4			65	404.3	373.2	93	221–223	224–226 [31]
5			160	386.9	145.1	89	150–152	149–151 [51]
6			150	369.5	147.8	85	249–250	253–256 [47]
7			75	386.9	320	92	213–215	209–210 [47]
8			90	395.6	263.8	91	172–174	173–176 [31]
9			50	386.9	464.3	89	133–135	129–132 [31]

Table 3 (continued)

Entry	Nitrile	Product	Time (min)	TON	TOF (h^{-1})	Yield[a] (%)	Obtained Melting point (°C)	Reported Melting point (°C)
10			130	373.9	172.6	86	210–213	212–214 [51]
11			60	373.9	373.9	86	111–113	114–116 [47]
12			75	395.6	316.5	91	257–260	260–262 [51]

[a]Isolated yield

It is well known that organic reactions are dependent on procedure conditions. Therefore in this regard, the various conditions including the amount of catalysts, nature of solvent and temperature were examined in the [2 + 3] cycloaddition reaction of benzonitrile with sodium azide for the synthesis of 5-phenyl-1H-tetrazole as model reaction, and the obtained results were summarized in Table 2. As shown in Table 2, the best results were obtained in the presence of 30 mg of ZrO-SB-APT@MCM-41 (Table 2, entry 3) or 25 mg of Cu-SB-APT@MCM-41 (Table 2, entry 12). No product was obtained in the absence of catalysts (Table 2, entry 1). Also, in order to study the solvent effect, the model reaction was examined in various solvents. As shown, the model reaction could proceed better in PEG-400. Finally, the effect of temperature was examined in the model reaction and the best results were obtained at 120 °C.

After the optimization of the reaction conditions, we extended the catalytic activity of ZrO-SB-APT@MCM-41 (Table 3) and Cu-SB-APT@MCM-41 (Table 4) for other nitrile derivatives including aromatic and aliphatic nitriles. Also, various benzonitrile derivatives bearing electron-donor and electron-withdrawing functional groups were investigated and all products were obtained in good yields and high TOF values. Dicyano substituted of aliphatic and aromatic nitriles such as malononitrile (Tables 3 and 4, entry 11), phthalonitrile (Tables 3 and 4, entry 7) and terephthalonitrile (Tables 3 and 4, entry 6) were also investigated which all of them afforded the monoaddition products. Therefore, these methodologies are effective for the synthesis of a wide range of tetrazol derivatives.

The chemo and homoselective oxidation of sulfides to sulfoxides were studied in the presence of ZrO-SB-APT@MCM-41 and Cu-SB-APT@MCM-41 (Scheme 4).

In order to obtain the reaction conditions, the oxidation of 2-phenylthioethanol was selected as a model substrate. The effect of different parameters such as the amount of catalysts and the nature of the solvent was examined in the model reaction (Table 5). Among the various conditions, 0.020 g of ZrO-SB-APT@MCM-41 under solvent-free conditions (Table 5, entry 3) or 0.0025 g of Cu-SB-APT@MCM-41 in ethyl acetate (Table 5, entry 1) appeared to be the best conditions for oxidation of 2-Phenylthioethanol to 2-(phenylsulfinyl)ethanol. Higher amount of catalysts did not change the amount of product and reaction time (Table 5, entries 3, 10 and 11).

The scop of catalytic activity of ZrO-SB-APT@MCM-41 and Cu-SB-APT@MCM-41 was explored in the oxidation of various sulfides. Therefore aliphatic and aromatic sulfides were examined and all products were obtained in excellent yields and TOF values. The obtained results are summarized in Tables 6 and 7. All sulfoxides were obtained in high purity without over oxidation or any by-product such as sulfon.

Selectivity in organic process are important from both green chemistry and industrial [55–60]. In order to indicate the chemoselectivity of these catalysts, other functional groups such as hydroxyl groups or olefin bands (that can compete in the oxidative reaction) were investigated in the oxidation of sulfides in the presence of ZrO-SB-APT@MCM-41 and Cu-SB-APT@MCM-41. As shown in Scheme 5, these functional groups are remained intact during the oxidation of sulfides to sulfoxides (Tables 6 and 7, entry 3) which confirmed the selectivity of these catalysts in oxidation of organosulfur compounds.

Homoselectivity is an interesting property of some organic reactions which can be observed in the same

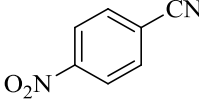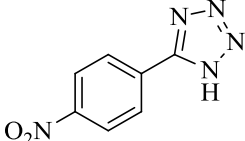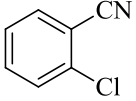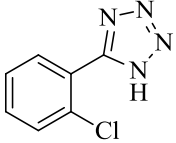**Table 4** Synthesis of tetrazoles in the presence of Cu-SB-APT@MCM-41
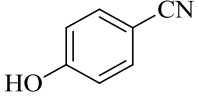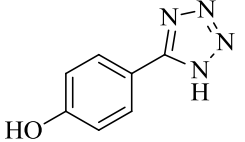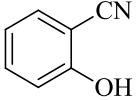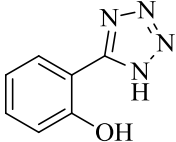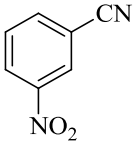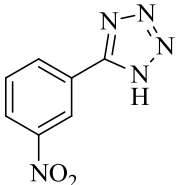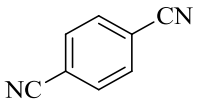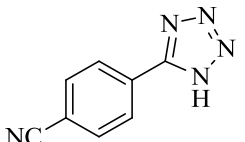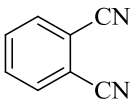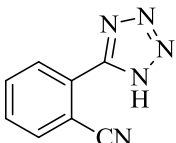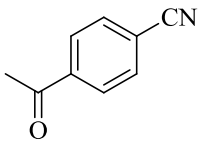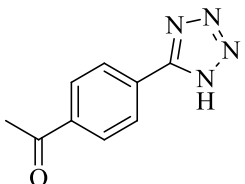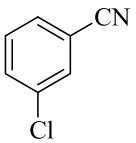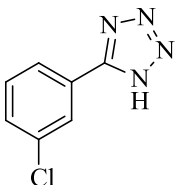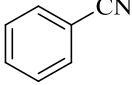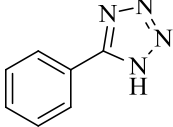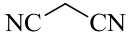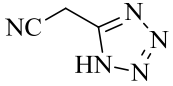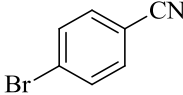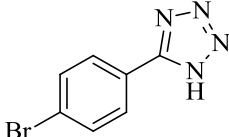
Entry	Nitrile	Product	Time (min)	TON	TOF (h^{-1})	Yield[a] (%)	Obtained melting point (°C)	Reported melting point (°C)
1			60	16.9	16.9	93	217–219	218–220 [51]
2			130	15.6	7.2	86	180–182	180–183 [31]
3			10	17.1	102.5	94	229–231	230–232 [51]
4			20	16.7	50.2	92	222–224	224–226 [31]
5			30	17.6	35.3	97	148–150	149–151 [51]
6			30	16.5	33.1	91	251–253	253–256 [47]
7			15	16.2	64.7	89	209–212	209–210 [47]
8			95	16.4	10.3	90	170–173	173–176 [31]
9			15	16.9	67.6	93	130–131	129–132 [31]

Table 4 (continued)

Entry	Nitrile	Product	Time (min)	TON	TOF (h^{-1})	Yield[a] (%)	Obtained melting point (°C)	Reported melting point (°C)
10	(phenyl-CN)	(5-phenyl-1H-tetrazole)	55	16.7	18.2	92	212–214	212–214 [51]
11	NC—CN	(cyanomethyl tetrazole)	25	15.8	63.3	87	113–114	114–116 [47]
12	(4-bromophenyl-CN)	(4-bromophenyl tetrazole)	50	16	19.2	88	257–260	260–262 [51]

[a]Isolated yield
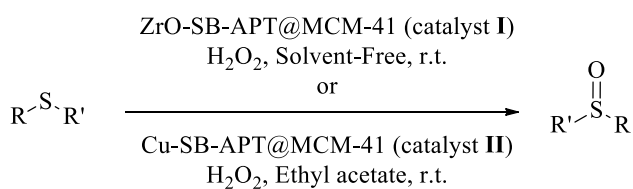
Scheme 4 Oxidation of sulfides in the presence of ZrO-SB-APT@MCM-41 or Cu-SB-APT@MCM-41

$$R \overset{S}{\diagdown} R' \xrightarrow[\substack{\text{Cu-SB-APT@MCM-41 (catalyst II)} \\ \text{H}_2\text{O}_2, \text{Ethyl acetate, r.t.}}]{\substack{\text{ZrO-SB-APT@MCM-41 (catalyst I)} \\ \text{H}_2\text{O}_2, \text{Solvent-Free, r.t.} \\ \text{or}}} R' \overset{O}{\underset{\|}{\overset{\|}{S}}} R$$

functional groups [57–60]. The homoselectivity of this procedure was examined in the oxidation of thianthrene which has two sulfides functional groups with same position in its structure. As shown in Scheme 6, this procedure

was shown a good homoselectivity in the oxidation of thianthrene.

3.4 Reusability of the catalysts
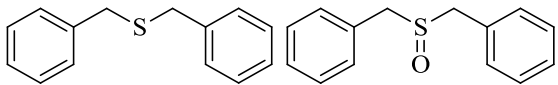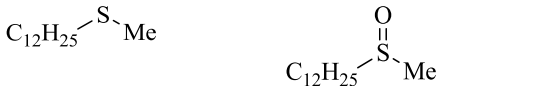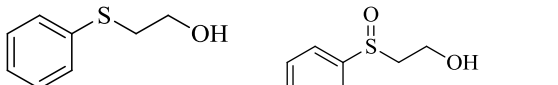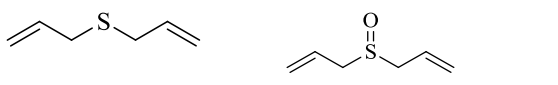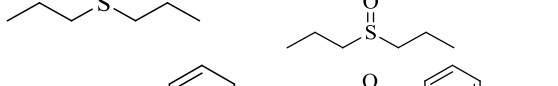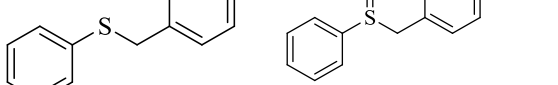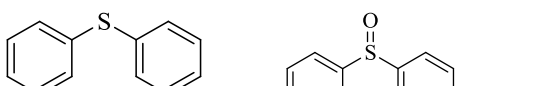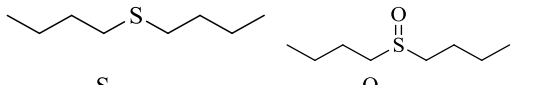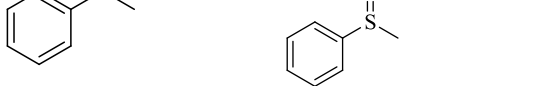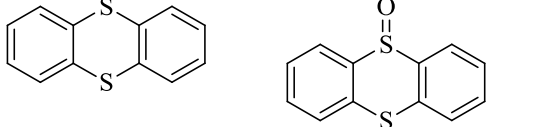
In order to show the stability and reusability of ZrO-SB-APT@MCM-41 and Cu-SB-APT@MCM-41, the reusability of Cu-SB-APT@MCM-41 was studied in the synthesis of 5-phenyl-1H-tetrazole and also the reusability of ZrO-SB-APT@MCM-41 was studied in the oxidation of methyl phenyl sulfide. For this purpose, at the end of each reaction, the catalysts were isolated by centrifugation and further used in the next run under optimized conditions. The obtained results from reusability of these catalysts were summarized in Fig. 11. It was found that these catalysts can be reused

Table 5 Optimization reaction conditions for the oxidation of sulfides in the presence of ZrO-SB-APT@MCM-41 (catalyst **I**) or Cu-SB-APT@MCM-41 (catalyst **II**)

Entry	Catalyst	Amount of catalyst (mg)	Solvent	Time (min)	Yield (%)[a]
1	–	–	Solvent-free	130	Trace
2	Catalyst I	10	Solvent-free	80	76
3	Catalyst I	20	Solvent-free	60	87
4	Catalyst I	30	Solvent-free	45	91
5	Catalyst I	20	Ethyl acetate	90	49
6	Catalyst I	20	Ethanol	110	51
9	Catalyst I	20	Dichloromethane	150	37
10	Catalyst I	2.5	Ethyl acetate	10	88
11	Catalyst II	5	Ethyl acetate	10	90
12	Catalyst II	10	Ethyl acetate	7	93
13	Catalyst II	2.5	Dichloromethane	15	56
14	Catalyst II	2.5	Acetonitrile	10	62
15	Catalyst II	2.5	Solvent-free	20	80

[a]Isolated yield

Table 6 Oxidation of sulfides to sulfoxides in the presence of ZrO-SB-APT@MCM-41

Entry	Product	Time (min)	TON	TOF (h^{-1})	Yield[a] (%)	Obtained Melting point (°C)	Reported Melting point (°C)
1		25	560.0	1344	84	130–132	134–136 [52]
2	C$_{12}$H$_{25}$–S–Me	30	620.0	1240	93	61–63	61–64 [48]
3		60	520.0	520	78	Oil	Oil [53]
4		35	606.7	1040	91	Oil	Oil [53]
5		80	620.0	465	93	Oil	Oil [48]
6		55	593.3	647.3	89	114–115	116–120 [54]
7		180	573.3	573.3	86	70–72	68–70 [55]
8		30	600.0	1200	90	Oil	Oil [52]
9		45	606.7	808.9	91	33–34	30–32 [48]
10		300	533.3	106.7	80	139–141	142–145 [54]

[a]Isolated yield

up to 6 runs. As shown, these catalysts did not show any significant change in their activity after 6 runs.

3.5 Characterization of recycled catalysts

The structural stability of recovered ZrO-SB-APT@MCM-41 and recovered Cu-SB-APT@MCM-41 were characterized by SEM, EDS, WDX, XRD, FT-IR and AAS technique.

The comparison of FT-IR spectra of recovered and fresh catalysts are shown in Fig. 12, which any change of catalysts after recovering was not observed. These results are a good witness for stability of ZrO-SB-APT@MCM-41 and Cu-SB-APT@MCM-41 after recycling, therefore these catalysts can

be recovered and reused for several runs without any change in their structure.

The morphology and particle size of Cu-SB-APT@MCM-41 and ZrO-SB-APT@MCM-41 after recycling have been compared with fresh of them by SEM technique. The SEM images of recovered Cu-SB-APT@MCM-41 and recovered ZrO-SB-APT@MCM-41 are shown in Fig. 13. As shown in Fig. 13, the size and morphology of these catalysts after recycling were shown a good similarly to fresh catalysts.

Table 7 Synthesis of tetrazoles in the presence of Cu-SB-APT@MCM-41

| Entry	Sulfide	Product	Time (min)	TON	TOF (h^{-1})	Yield[a] (%)	Obtained Melting point (°C)	Reported Melting point (°C)
1	dibenzyl sulfide	dibenzyl sulfoxide	11	160.0	872.7	88	131–133	134–136 [52]
2	$C_{12}H_{25}$–S–Me	$C_{12}H_{25}$–S(O)–Me	8	169.1	1268.2	93	62–64	61–64 [48]
3	PhS–CH₂CH₂OH	PhS(O)–CH₂CH₂OH	10	158.2	949.1	87	Oil	Oil [53]
4	diallyl sulfide	diallyl sulfoxide	7	156.4	1340.2	86	Oil	Oil [53]
5	dipropyl sulfide	dipropyl sulfoxide	8	170.9	1281.8	94	Oil	Oil [48]
6	benzyl phenyl sulfide	benzyl phenyl sulfoxide	10	161.8	970.9	89	113–115	116–120 [54]
7	diphenyl sulfide	diphenyl sulfoxide	100	163.6	98.2	90	69–71	68–70 [55]
8	dibutyl sulfide	dibutyl sulfoxide	50	160.0	192	88	Oil	Oil [52]
9	methyl phenyl sulfide	methyl phenyl sulfoxide	13	170.9	788.8	94	33–34	30–32 [48]

[a] Isolated yield

3.6 Leaching study of the catalysts

Metal leaching of Cu-SB-APT@MCM-41 and ZrO-SB-APT@MCM-41 was studied by AAS analysis and poisoning test. In this regard, [2 + 3] cycloaddition reaction of benzonitrile with NaN_3 was repeated under optimized condition (Tables 3 and 4, entries 10) and the catalysts were isolated from reaction solution after completion of each reaction. Based on obtained results from AAS analysis, amount of zirconium in fresh and recovered catalyst (ZrO-SB-APT@MCM-41) were found to be 0.076×10^{-3} mol g^{-1} and 0.1×10^{-3} mol g^{-1}, respectively. In the other hand, the amount of copper in fresh and recovered catalyst (Cu-SB-APT@MCM-41) were found to be 2.2×10^{-3} mol g^{-1} and 1.96×10^{-3} mol g^{-1}, respectively. Exact amount of metal content in recovered catalysts is shown a good agreement to fresh catalyst, which was confirmed the heterogeneity nature of these catalysts.

Poisoning test is a useful method for heterogeneity/homogeneity nature of catalysts which can be studied by PVP or mercury [61, 62]. Therefore oxidation of dibenzylsulfane in the presence of PVP and Cu-SB-APT@MCM-41 or ZrO-SB-APT@MCM-41 was performed under solvent-free conditions at room temperature. In these experiments, 86% of (sulfinylbis(methylene))dibenzene was obtained in the presence of Cu-SB-APT@MCM-41 after 10 min and 85% of this product was obtained in the presence of ZrO-SB-APT@MCM-41 after 30 min. These results are shown good agreement with obtained results in the absent of PVP (Tables 6 and 7, entries 1) which proves that Cu-SB-APT@MCM-41 and ZrO-SB-APT@MCM-41 have heterogeneous nature.

3.7 Comparison study of the catalysts

In order to evaluate the efficiency of ZrO-SB-APT@MCM-41 and Cu-SB-APT@MCM-41, in the oxidation of methyl phenyl
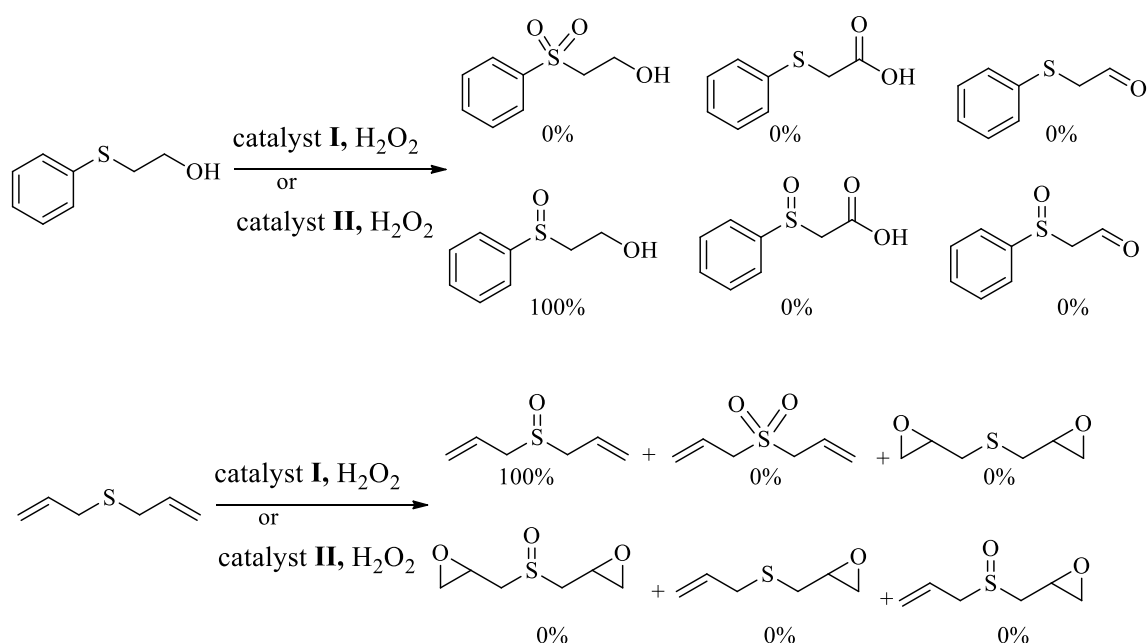
Scheme 5 Chemoselectivity oxidation of sulfides using ZrO-SB-APT@MCM-41 and Cu-SB-APT@MCM-41

Scheme 6 Homoselectivity oxidation of thianthrene in the presence of ZrO-SB-APT@ MCM-41
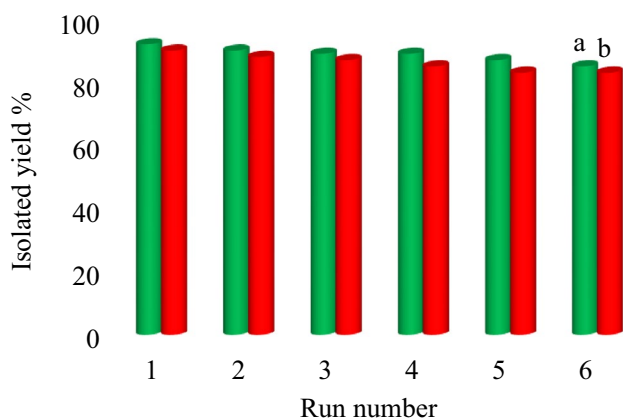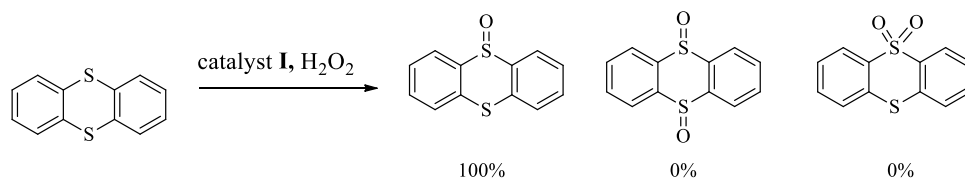
Fig. 11 The reusability of Cu-SB-APT@MCM-41 in the synthesis of 5-phenyl-1H-tetrazole (a) and the reusability of ZrO-SB-APT@ MCM-41 in the oxidation of methyl phenyl sulfide (b)

sulfide to (methylsulfinyl)benzene, this work was compared with previously reported catalysts in the work of literatures (Table 8). It can be seen that described catalysts in this work are superior to others in terms of efficiency and reaction time.

The products were obtained in higher yields and TOF values when ZrO-SB-APT@MCM-41 or Cu-SB-APT@MCM-41 was used as catalyst.

4 Conclusions

In conclusions, we modified MCM-41 and two Schiff-base complexes of copper and zirconium were stabilized on its surface (ZrO-SB-APT@MCM-41 and Cu-SB-APT@ MCM-41). These catalysts were characterized by XRD, TGA, TEM, TF-IR, SEM, EDS, WDX, BET and AAS techniques. Then, catalytic activities of these catalysts were described in the synthesis of tetrazole derivatives and also in the chemo and homoselective oxidation of sulfides to sulfoxides. All the products were obtained in good to excellent yields and high TOF values. Also, the reusability of these catalysts was described which shows good reusability in described reactions. The recovered catalysts were characterized by SEM, FT-IR and AAS analysis which shown an excellent agreement with fresh catalysts.

Fig. 12 FT-IR spectra of Cu-SB-APT@MCM-41 (a), recovered Cu-SB-APT@MCM-41 (b), ZrO-SB-APT@MCM-41 (c), and recovered ZrO-SB-APT@MCM-41 (d)

Fig. 13 SEM images of recovered Cu-SB-APT@MCM-41 (**a**) and recovered ZrO-SB-APT@MCM-41 (**b**)

Table 8 Comparison of ZrO-SB-APT@MCM-41 or Cu-SB-APT@MCM-41 in the oxidation of methyl phenyl sulfide with previously reported procedures
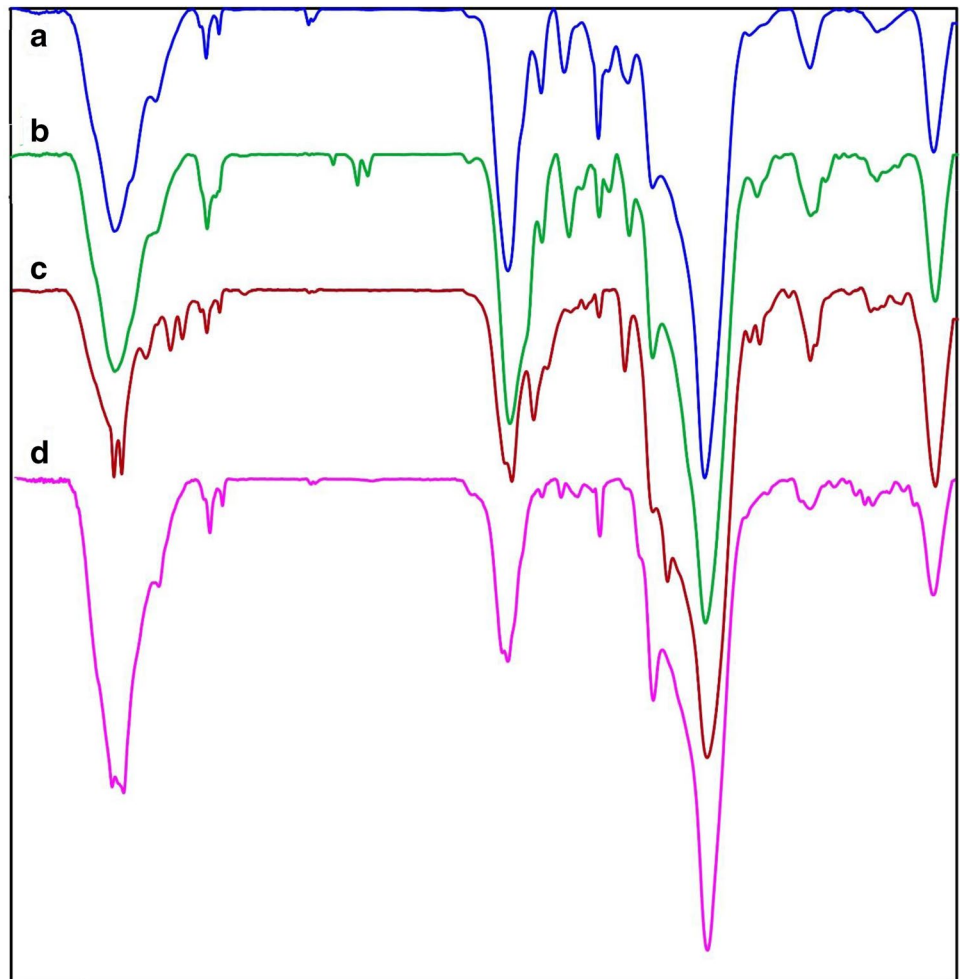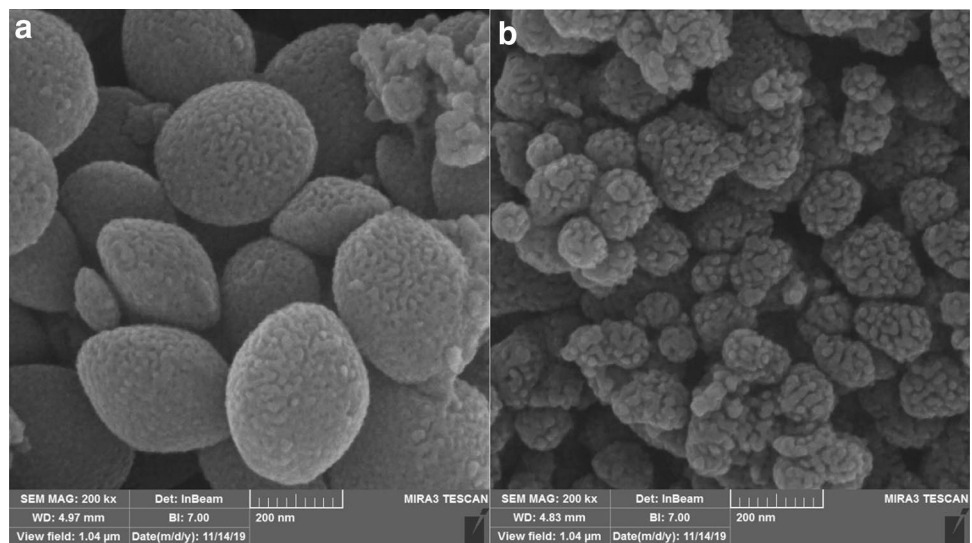
Entry	Catalyst	Time (min)	Yield(%) [References]
1	DSA@MNPs	360	98 [63]
2	Polymer-anchored Cu(II)	180	90 [64]
3	Cu-SPATB/Fe$_3$O$_4$	95	98 [65]
4	Cd-salen-MCM-41	150	98 [66]
5	VO$_2$F(dmpz)$_2$	300	95 [67]
6	Ni-salen-MCM-41	156	95 [66]
7	TsOH, PhI(OAc)$_2$	240	88 [68]
8	Ni-dithizone@boehmite	80	96 [53]
9	SVA	5	94 [69]
10	M@PEI@Br	120	87.3 [70]
11	Cu-SBTU@MCM-41	70	97 [71]
12	2NaBO$_3$·4H$_2$O, SSA, KBr, wet SiO$_2$ (50% w/w)	240	80 [72]
13	Cu–Adenine@boehmite	60	98 [48]
14	ZrO-SB-APT@MCM-41	45	91 [this work]
15	Cu-SB-APT@MCM-41	13	94 [this work]

References

1. J. Govan, K.Y. Gunko, Nanomaterials **4**, 222 (2014)
2. T. Baran, N. Yılmaz Baran, A. Menteş, Appl. Organomet. Chem. **32**, e4075 (2018)
3. T. Baran, Ultrason. Sonochem. **45**, 231 (2018)
4. D. Wang, D. Astruc, Chem. Rev. **114**, 6949 (2014)
5. S. Shylesh, V. Schünemann, W.R. Thiel, Angew. Chem. Int. Ed. **49**, 3428 (2010)
6. R.R. Langeslay, D.M. Kaphan, C.L. Marshall, P.C. Stair, A.P. Sattelberger, M. Delferro, Chem. Rev. **119**, 2128 (2019)
7. T. Baran, N. Yılmaz Baran, A. Menteş, J. Mol. Struct. **1160**, 154 (2018)
8. P. Ju, S. Wu, Q. Su, X. Li, Z. Liu, G. Li, Q. Wu, J. Mater. Chem. A **7**, 2660 (2019)
9. T. Baran, Carbohydr. Polym. **195**, 45 (2018)
10. Y. Rangraz, F. Nemati, A. Elhampour, New J. Chem. **42**, 15361 (2018)
11. A. Ghorbani-Choghamarani, M. Hajjami, B. Tahmasbi, N. Noori, J. Iran. Chem. Soc. **13**, 2193 (2016)
12. J.K. Anjali, K. Sreekumar, Catal. Lett. **149**, 1952 (2019)
13. V. Polshettiwar, R.S. Varma, Green Chem. **12**, 743 (2010)
14. T. Baran, N. Yılmaz Baran, A. Menteş, Int. J. Biol. Macromol. **115**, 249 (2018)
15. D. Ma, Y. Wang, A. Liu, S. Li, C. Lu, C. Chen, Catalysts **8**, 404 (2018)
16. M. Nikoorazm, A. Ghorbani-Choghamarani, A. Panahi, B. Tahmasbi, N. Noori, J. Iran. Chem. Soc. **15**, 181 (2018)
17. C.W. Lim, I.S. Lee, Nano Today **5**, 412 (2010)
18. V. Polshettiwar, R. Luque, A. Fihri, H. Zhu, M. Bouhrara, J.-M. Basset, Chem. Rev. **111**, 3036 (2011)
19. A. Ghorbani-Choghamarani, B. Tahmasbi, R.H.E. Hudson, A. Heidari, Microporous Mesoporous Mater. **284**, 366 (2019)
20. B. Karimi, M. Tavakolian, F. Mansouri, H. Vali, A.C.S. Sustain. Chem. Eng. **7**, 3811 (2019)
21. E. Gross, F. Dean Toste, G.A. Somorjai, Catal. Lett. **145**, 126 (2015)
22. B. Tahmasbi, A. Ghorbani-Choghamarani, Catal. Lett. **147**, 649 (2017)
23. H. Veisi, A. Nikseresht, N. Ahmadi, K. Khosravi, F. Saeidifar, Polyhedron **162**, 240 (2019)
24. Z.B. Shifrina, V.G. Matveeva, L.M. Bronstein, Chem. Rev. (2019). https://doi.org/10.1021/acs.chemrev.9b00137
25. S.Y. Chong, T.T. Wang, L.C. Cheng, H.Y. Lv, M. Ji, Langmuir **35**, 495 (2019)
26. T.T. Nguyen, X.-T.T. Nguyen, T.-L.H. Nguyen, P.H. Tran, ACS Omega **4**, 368 (2019)
27. A. Ghorbani-Choghamarani, B. Tahmasbi, N. Noori, S. Faryadi, Comptes Rendus Chim. **20**, 132 (2017)
28. R.M. Ansari, B.R. Bhat, Chem. Phys. **517**, 155 (2019)
29. V.B. Saptal, M.V. Saptal, R.S. Mane, T. Sasaki, B.M. Bhanage, ACS Omega **4**, 643 (2019)
30. A. Ghorbani-Choghamarani, M. Nikoorazm, H. Goudarziafshar, B. Tahmasbi, Bull. Korean Chem. Soc. **40**, 1388 (2009). https://doi.org/10.1002/chin.200945034
31. B. Tahmasbi, A. Ghorbani-Choghamarani, Appl. Organomet. Chem. **31**, e3644 (2017)
32. K. Bahrami, M. Khodamorady, Catal. Lett. **149**, 688 (2019)
33. S.A. Idris, S.R. Harvey, L.T. Gibson, J. Hazard. Mater. **193**, 171 (2011)
34. M. Nikoorazm, N. Noori, B. Tahmasbi, S. Faryadi, Transit. Met. Chem. **42**, 469 (2017)
35. G. Maria, A.-I. Stoica, I. Luta, D. Stirbet, G.L. Radu, Microporous Mesoporous Mater. **162**, 80 (2012)
36. Y. Sun, X.-W. Liu, W. Su, Y. Zhou, L. Zhou, Appl. Surf. Sci. **253**, 5650 (2007)
37. A. Benhamou, J.P. Basly, M. Baudu, Z. Derriche, R. Hamacha, J. Colloid Interface Sci. **404**, 135 (2013)
38. M. Nikoorazm, A. Ghorbani-Choghamarani, N. Noori, B. Tahmasbi, Appl. Organomet. Chem. **30**, 843 (2016)
39. M. Nikoorazm, A. Ghorbani-Choghamarani, F. Ghorbani, H. Mahdavi, Z. Karamshahi, J. Porous Mater. **22**, 261 (2015)
40. M. Abdollahi-Alibeik, M. Pouriayevali, Catal. Commun. **22**, 13 (2012)
41. Y. Huang, W. Hao, G. Ding, M.-Z. Cai, J. Organomet. Chem. **715**, 141 (2012)
42. S. Rojas-Buzo, P. García-García, A. Corma, Catal. Sci. Technol. **9**, 146 (2019)
43. N. Yan, C. You, M. Cai, J. Organomet. Chem. **897**, 161 (2019)
44. H. Veisi, T. Tamoradi, B. Karmakar, New J. Chem. **43**, 10343 (2019)
45. M. Bharathi, S. Indira, G. Vinoth, K. Shanmuga Bharathi, J. Porous Mater. **26**, 1377 (2019)
46. S. Molaei, M. Ghadermazi, Appl. Organomet. Chem. **33**, e4854 (2019)
47. M. Nikoorazm, A. Ghorbani-Choghamaranai, M. Khanmoradi, P. Moradi, J. Porous Mater. **25**, 1831 (2018)
48. A. Ghorbani-Choghamarani, P. Moradi, B. Tahmasbi, Polyhedron **163**, 98 (2019)
49. T. Tamoradi, M. Ghadermazi, A. Ghorbani-Choghamarani, Catal. Lett. **148**, 857 (2018)
50. T. Tamoradi, M. Ghadermazi, A. Ghorbani-Choghamarani, New J. Chem. **42**, 5479 (2018)
51. A. Ghorbani-Choghamarani, P. Moradi, B. Tahmasbi, RSC Adv. **6**, 56638 (2016)
52. A. Ghorbani-Choghamarani, P. Moradi, B. Tahmasbi, RSC Adv. **6**, 56458 (2016)

53. A. Ghorbani-Choghamarani, P. Moradi, B. Tahmasbi, J. Iran. Chem. Soc. **16**, 511 (2019). https://doi.org/10.1007/s13738-018-1526-5

54. A. Ghorbani-Choghamarani, H. Goudarziafshar, M. Nikoorazm, S. Yousefi, Lett. Org. Chem. **6**, 335 (2009)

55. M. Safaiee, M. Moeinimehr, M.A. Zolfigol, Polyhedron **170**, 138 (2019)

56. M. Zolfigol, F. Shirini, A. Choghamarani, Synthesis (Stuttg). **2006**, 2043 (2006)

57. G. Chehardoli, M.A. Zolfigol, Phosphorus, Sulfur Silicon Relat. Elem. **185**, 193 (2010)

58. K. Amani, M.A. Zolfigol, A. Ghorbani-Choghamarani, M. Hajjami, Monat. Chem. Chem. Mon. **140**, 65 (2009)

59. A. Hasaninejad, G. Chehardoli, M.A. Zolfigol, A. Abdoli, Phosphorus Sulfur Silicon Relat. Elem. **186**, 271 (2011)

60. M.A. Zolfigol, K. Amani, A. Ghorbani-Choghamarani, M. Hajjami, R. Ayazi-Nasrabadi, S. Jafari, Catal. Commun. **9**, 1739 (2008)

61. T. Baran, E. Açıksöz, A. Menteş, J. Mol. Catal. A: Chem. **407**, 47 (2015)

62. B. Tahmasbi, A. Ghorbani-Choghamarani, New J. Chem. **43**, 14485 (2019)

63. A. Ghorbani-Choghamarani, H. Rabiei, B. Tahmasbi, B. Ghasemi, F. Mardi, Res. Chem. Intermed. **42**, 5723 (2016). https://doi.org/10.1007/s11164-015-2399

64. S.M. Islam, A.S. Roy, P. Mondal, K. Tuhina, M. Mobarak, J. Mondal, Tetrahedron Lett. **53**, 127 (2012)

65. A. Ghorbani-Choghamarani, B. Tahmasbi, P. Moradi, N. Havasi, Appl. Organomet. Chem. **30**, 619 (2016)

66. M. Nikoorazm, A. Ghorbani-Choghamarani, H. Mahdavi, S.M. Esmaeili, Microporous Mesoporous Mater. **211**, 174 (2015)

67. S. Hussain, D. Talukdar, S.K. Bharadwaj, M.K. Chaudhuri, Tetrahedron Lett. **53**, 6512 (2012)

68. C. Yu, C.-X. Guo, C.-L. Zhong, Z.-F. Diao, L.-N. He, Tetrahedron Lett. **55**, 1818 (2014)

69. M.A. Zolfigol, A. Khazaei, M. Safaiee, M. Mokhlesi, R. Rostamian, M. Bagheri, M. Shiri, H.G. Kruger, J. Mol. Catal. A: Chem. **370**, 80 (2013)

70. Y. Hu, W. Ma, M. Tao, X. Zhang, X. Wang, X. Wang, L. Chen, J. Appl. Polym. Sci. **135**, 46036 (2018)

71. M. Nikoorazm, M. Ghobadi, Silicon **11**, 983 (2019)

72. D. Habibi, M.A. Zolfigol, M. Safaiee, A. Shamsian, A. Ghorbani-Choghamarani, Catal. Commun. **10**, 1257 (2009)